Research Square

Preprints are preliminary reports that have not undergone peer review.
They should not be considered conclusive, used to inform clinical practice,
or referenced by the media as validated information.

Unravelling the Endogenous Chemical Stability of Multi-Source Ashes: Decoupling Chemical Sequestration from Physical Encapsulation for Sustainable Construction

Arezou Babaahmadi

arezou.ahmadi@chalmers.se

Chalmers University of Technology

Baodong Li

Chalmers University of Technology

Samuel J. Armistead

Sebastien Rauch

Liming Huang

Article

Keywords: Leaching behaviour, dissolution, heavy metals, biomass ash, municipal solid waste incineration ash, volcanic ash

Posted Date: April 22nd, 2026

DOI: https://doi.org/10.21203/rs.3.rs-9343875/v1

License: This work is licensed under a Creative Commons Attribution 4.0 International License. Read Full License

Additional Declarations: There is **NO** Competing Interest.

Abstract

Waste-derived ashes are emerging as promising supplementary cementitious materials, yet their environmental safety is constrained by poorly understood stabilization mechanisms. This study systematically investigates the leaching behaviour and endogenous stabilization capacity of three representative multi-source ashes, including biomass ash (BA), municipal solid waste incineration ash (MA), and volcanic ash (VA), through a long-term rotation-based kinetic leaching approach designed to decouple chemical sequestration from physical encapsulation. Results reveal that leaching behaviour is strongly governed by the chemical environment. Under simulated cementitious conditions, heavy metal concentrations were suppressed by 1–2 orders of magnitude. This immobilization is attributed to a dual mechanism of rapid hydroxide precipitation and progressive structural incorporation into hydration products. The continuous Ca^{2+} consumption and hydration phase formation confirm that ashes act as reaction sinks for both major and trace elements. Mineralogical analysis shows significant amorphous phase dissolution and formation of stable hydrates. Kinetic modelling indicates that leaching is predominantly diffusion-controlled in water systems, while stage-dependent analysis reveals a dynamic competition between dissolution and immobilization processes. Overall, the findings establish that heavy metal stabilization in waste-derived supplementary cementitious materials is an intrinsic chemical property, providing a mechanistic basis for their safe and sustainable utilization in low-carbon construction materials.

1. Introduction

Cement production is the third largest source of anthropogenic CO_2 emissions, contributing approximately 8% of global emissions [1]. To mitigate the environmental impact of concrete production, supplementary cementitious materials (SCMs) have been widely adopted, with waste-derived SCMs offering the dual benefits of decarbonization and circular economy promotion [2]. However, conventional SCMs such as fly ash, blast furnace slag, and silica fume are increasingly constrained by supply limitations, spurring interest in emerging alternatives like reactive ashes [3–5]. Despite energy recovery during incineration, residual municipal solid waste incineration fly ash (MA) is often landfilled, highlighting the need for sustainable utilization strategies [6]. Similarly, biomass fly ash (BA), a by-product of power generation, is produced in significant quantities and exhibits promising reactivity [7, 8]. Volcanic ash (VA), formed through ash-gas interactions, has demonstrated potential reactivity as SCM [9, 10].

Nevertheless, the variability in chemical composition, alkalinity, strength development, and hazardousness of these alternative ashes necessitates further research to enable their broader application in construction. While existing literature has extensively explored the properties and durability of emerging SCMs, their potential leaching risks of heavy metals remain underexplored [11–13]. For example, most kinds of MA are still classified as hazardous waste due to its high concentrations of heavy metals and unwanted salts [14]. BA is often treated as controlled waste under strict regulations across the EU and other regions due to its high leaching risk [15, 16]. VA, too, poses environmental hazards during and after volcanic eruptions [9, 17]. Consequently, the hazardous nature of these ashes must be systematically assessed to ensure their safe recycling as SCMs to prevent environmental contamination.

Leaching, the process by which elements are released from solid materials into solution, plays a critical role in assessing the environmental safety [18]. In cementitious systems, leaching is often perceived as an environmental concern due to the potential release of heavy metals and other harmful elements [19, 20]. The

leaching mechanism of different ashes still remains studied, especially in different leaching conditions considering the high pH environment of cementitious materials [21, 22]. However, the lack of harmonized leaching criteria across different jurisdictions creates uncertainty in how waste-derived SCMs are classified [23]. Currently, methods for assessing the stability of SCMs mainly focus on short-term compliance batch tests (TCLP) and long-term monolithic diffusion tests (Tank test) [24]. However, batch tests are inadequate for characterizing the slow, multi-stage kinetics of heavy metal release and secondary phase formation, while Tank test primarily reflects the physical embedding effect of blocky samples after 28 days of curing, masking the essential chemical interaction between heavy metals and mineral phases during hydration [25]. To eliminate the interference of physical structure, this paper innovatively adopts a long-period sampling strategy applied to a rotation system. This method ensures that heavy metals maintain sufficient contact area with the active powder throughout the hydration cycle of 1–90 days, thereby accurately quantifying the contribution of the novel SCM to the chemical binding of heavy metals during the hydration process. This ensures that our approach remains scientifically rigorous while capturing key dissolution and transformation processes of SCMs.

In this study, we investigate the leaching behaviour of BA, MA, and VA, three SCMs with distinct mineralogical compositions and dissolution characteristics. To bridge the gap between compositional analysis and leaching behaviour, we employ a structured kinetic leaching approach that tracks element release over time, considering both initial dissolution rates and long-term phase transformations. By coupling mineralogical analysis with kinetic modelling, we identify the dominant leaching mechanisms at different stages, distinguishing between depletion-controlled, dissolution-controlled, and diffusion-controlled processes. This study does not seek to replace standard leaching tests but rather to provide a complementary approach that links hydration, phase stability, and element mobility in SCMs. The findings are beneficial to the safe and sustainable application of multi-source ashes as SCMs, contributing to advancements in low-carbon construction practices.

2. Materials and methods

2.1 Raw materials

Ash derived from MSWI and wood pellet incineration for energy production was acquired, hereby known MA and BA, respectively. VA was sourced from a volcanic site near Reykjavik, Iceland. All binder materials were stored in opaque, sealed containers to prevent alterations in their chemical characteristics over time. The chemical compositions of the ashes, determined using Inductively Coupled Plasma Mass Spectrometry (ICP-MS, ICAP Q, Thermo Fischer Scientific) equipped with a FAST sample introduction system (Elemental Scientific) and using He as collision gas, are summarized in Table 1. BA and VA exhibited high SiO_2 contents, while that of MA was only 5.97%. Conversely, MA displayed the highest CaO content among the samples, reaching 40.7%. The concentrations of heavy metals varied considerably across the ashes. For instance, MA showed notably high levels of MnO (4.98%), while the ZnO contents of BA reached 1.10%, which could have implications for its behaviour in both hydration and leaching scenarios. Generally, due to the high contents of heavy metals, the leaching risk of these studied ashes cannot be ignored.

Table 1
Chemical compositions of raw materials, wt%

Chemical compositions	SiO_2	Al_2O_3	Fe_2O_3	CaO	Na_2O	K_2O	MgO	LOI*	CuO	Cr_2O_3	ZnO
BA	41.00	8.98	2.07	19.15	1.44	1.25	1.70	9.49	0.18	0.08	1.10
MA	5.97	1.42	4.28	40.70	0.45	8.77	8.74	17.55	0.02	0.04	0.25
VA	48.30	14.60	13.25	11.95	2.10	0.15	7.44	-0.52	0.22	0.03	0.01

2.2 Experimental design

To establish a baseline for pozzolanic activity and its implications for leaching behaviour, the Frattini test was conducted following SS-EN 196-5:2011. This method monitors the dissolution of Ca^{2+} and OH^- over time, key indicators of pozzolanic reactivity in binders [26]. A liquid-to-solid ratio of 5:1 was selected for these tests, and all experiments were performed in triplicate. Each test utilized 15 ml Falcon tubes containing 7.5 ml of ultrapure water. The tubes were pre-heated to 40°C in a Thermo Scientific Heratherm Compact Microbiological Incubator equipped with a vertical tube rack. Once the water equilibrated to 40°C, individual Falcon tubes were removed, and the binder mix was added, followed by 20 seconds of vigorous shaking. The tubes were quickly sealed with tight caps and Bemis Parafilm to minimize exposure to ambient conditions, then returned to the incubator at 40°C. Samples were analysed at 1, 7, and 28 d. Conductivity was measured using a VWR HCO 304 handheld conductivity meter, while ionic concentrations of Ca^{2+} were determined using an Ionic Chromatography System (ICS-900, Dionex).

Building upon the pozzolanicity assessment, the leaching behaviour of the binders was evaluated using a scaled-down setup adapted from SS-EN 12457-2. This approach allowed for the systematic investigation of element release under conditions relevant to cementitious systems. The experimental configuration involved 15 ml Falcon tubes containing 7.5 ml of leachate solution and 1.5 g of solid material, compared to the standard setup's 1 L containers (900 ml solution and 90 g solid). For this study, binders composed of 100% waste-derived pozzolanic materials were tested. Two sets of samples were prepared: (i) Using ultrapure water as the leachate. (ii) Using a saturated $Ca(OH)_2$ solution to simulate pozzolanic reaction conditions. The $Ca(OH)_2$ solution was prepared by dissolving 1.31 g of CaO in 1 L of ultrapure water with continuous stirring at 300 rpm for 4 hours, yielding a saturated solution with 1.78 g/L of $Ca(OH)_2$. In Falcon tubes, 7.5 ml of each leachate solution was added to 1.5 g of binder, sealed with caps and Bemis Parafilm. Agitation was achieved using a Fisher Scientific Mini Tube Rotator at 10 rpm, and leaching tests were performed at 20°C. Sampling was conducted at 1, 7, 14, 28, and 90 days, with all tests performed in triplicate. Ions in the leachate were analysed ICP-MS (ICAP Q, Thermo Fischer Scientific) equipped with a FAST sample introduction system (Elemental Scientific) and using He as collision gas. After the final sampling, the remaining solution was decanted, and the solid residues were placed in 15 mm Petri dishes. Isopropyl alcohol was immediately added to the residues to halt further hydration reactions.

2.3 Characterization methods

Mineralogical phases in the binders were quantitatively analysed using X-ray Diffraction (XRD, Bruker D8 Discover). To minimize particle orientation effects, the binders were first ground using a Retsch PM 100 Ball Mill (500 rpm, 10 minutes) with 100 × 5 mm steel balls in a 25 ml grinding jar. Ground samples (90 days) were sieved

using a Pascall Engineering automatic sieve shaker, with < 63 μm fraction was used for analysis. For phase quantification, 5% by weight of high-purity Al_2O_3 was added as an internal standard. The standard was manually mixed into each sample for 2 minutes to ensure homogenous dispersion. The surface morphology of ashes was observed by scanning electron microscopy (SEM, FEI Quanta 200 FEG), coupled with Energy Dispersive X-ray Spectroscopy (EDS) to illustrate the heavy metal elemental distribution.

3. Results and discussion

3.1. Elemental leaching kinetics

3.1.1 Major elements

The leaching behaviours of major elements (Ca, Al, and Na) serves as a foundational chemical marker to distinguish between simple physical dissolution and active pozzolanic consumption. As shown in Fig. 1, the elemental concentration patterns are highly sensitive to the leaching medium, revealing the intrinsic reactivity of the multi-source ashes. In the ultrapure water system (Fig. 1a), MA exhibited a rapid and massive release of Ca, reaching a peak concentration within 1 day. This behaviour is attributed to the immediate hydrolysis of its substantial CaO content (40.7%) into $Ca(OH)_2$. Conversely, the Ca release from BA and VA was significantly lower and followed a moderate plateauing trend, reflecting the dissolution of their respective aluminosilicate glass phases. The introduction of a saturated $Ca(OH)_2$ solution (Fig. 1d) completely transformed the leaching kinetic landscape. For the BA and VA systems, aqueous Ca concentrations showed a progressive and significant decrease over the 90-day period. This phenomenon provides the "smoking gun" for pozzolanic activity: rather than merely leaching, the ash particles are actively consuming Ca^{2+} from the bulk solution to precipitate C-(A)-S-H gels. By maintaining the system in a continuously rotating powder state, we ensured that this chemical consumption was not masked by the formation of a passivating product layer, which often restricts ion transport in static or monolithic tests. Al release followed a pH-dependent amphoteric solubility curve. While Al leaching was limited in water (Fig. 1b), its initial solubility was higher in the alkaline $Ca(OH)_2$ environment (Fig. 1e). However, for BA and VA, the Al concentration subsequently declined, signifying its systematic incorporation into alumina-bearing secondary phases, such as C-A-S-H or ettringite-like structures. Na, acting as a conservative tracer for simple dissolution, reached a steady state almost immediately in both media, as it does not participate significantly in the formation of secondary hydration products under these conditions.

3.1.2 Heavy metals

The environmental safety of these ashes is fundamentally defined by the mobility of trace heavy metals (Cu, Cr, and Zn). A pivotal finding of the unobstructed kinetic study is the dramatic suppression of heavy metal leaching in the $Ca(OH)_2$ solution compared to water (Fig. 2). In deionized water, all ashes exhibited measurable leaching, with BA releasing exceptionally high levels of Zn (≈ 10–100 mg/L), consistent with its industrial origin and 1.10% ZnO content. However, when exposed to the $Ca(OH)_2$ solution (Fig. 2d-f), the concentrations of Cu, Cr, and Zn were suppressed by one to two orders of magnitude. For instance, Zn leaching from BA dropped to below 0.1 mg/L, which is a suppression factor exceeding 100 times. This immobilization is the result of a dual immobilization effect that occurs independently of physical encapsulation. (i) Chemical Precipitation: The high-pH environment (≈ 12.5) forces the immediate precipitation of heavy metals as highly insoluble hydroxides. (ii)

Structural Sequestration: More crucially, the ongoing formation of pozzolanic reaction products (identified as "reaction sinks" in the major element analysis) provides a high-surface-area chemical lock. By utilizing a rotation-based powder system, we demonstrate that this sequestration is an intrinsic chemical property of the ash's reaction with the alkaline environment. Even without the physical density of a concrete monolith, the ashes possess an endogenous capacity to chemically integrate hazardous ions into their maturing mineral lattice. This reinforces the scientific justification for the long-term rotation method, which isolates and quantifies the maximum chemical potential for stabilization.

3.2 Pozzolanic reactivity and leaching environment characterization

The characterization of the leaching environment is critical to understanding the chemical stimuli that trigger the endogenous stabilization of SCMs. The pozzolanic potential of BA, MA, and VA was first validated via the Frattini test (Fig. 3a), where all ashes exhibited a clear consumption of Ca^{2+} and OH^-, positioning them below the lime solubility isotherm. Notably, MA showed a rapid initial reactivity, likely driven by its high autogenous alkalinity, while BA and VA demonstrated a progressive "maturation" over 28 days. The dynamic evolution of pH and conductivity (Fig. 3b-e) reveals how the "unobstructed" rotation method maintains a consistent reaction front. In the $Ca(OH)_2$ system (Fig. 3c and e), the pH was effectively buffered at approximately 12.5, simulating the saturated pore solution of a concrete matrix. The subtle but steady decline in conductivity, particularly for the BA and VA systems, directly corresponds to the removal of mobile ions from the aqueous phase to form stable hydrate solids. By employing a continuously rotating batch system, we eliminated the development of "stagnant boundary layers" that often occur in static tests, ensuring that the measured conductivity drop reflects the intrinsic chemical consumption by the ash particles rather than localized saturation. This provides a more accurate representation of the material's "maximum chemical potential" to act as a reaction sink during the long-term hydration process.

3.3. Physicochemical evolution of ash residues

3.3.1 Mineralogical analysis

The mineralogical evolution of the multi-source ashes after 90 days leaching was systematically evaluated using XRD. As shown in Fig. 4, the transition from a raw matrix to a reacted cementitious system is clearly driven by the chemical environment. BA is initially composed of a dominant amorphous phase (69.0%), quartz (16.9%), gypsum (10.1%), and minor feldspar and carbonate. After 90 days of leaching, the mineralogical landscape undergoes a significant shift driven by phase dissolution. In the $Ca(OH)_2$ system, the amorphous content decreases to 48.7%. This dissolution of the glass phase triggers a relative enrichment of stable, non-reactive minerals; specifically, the quartz content appears to surge to 35.6% and feldspar to 11.3%. This apparent increase does not signify mineral formation but rather the loss of absolute mass from the unstable amorphous components. Notably, the gypsum phase in BA exhibits high environmental sensitivity, remaining stable in water (13.1%) but dissolving almost completely in the alkaline $Ca(OH)_2$ medium (2.5%). Despite the reduction in amorphous content, the Ca leaching results in Section 3.1 show that Ca concentrations in the CH group are actually slightly lower than in the water group, confirming that the alkaline medium triggers a "reaction sink" effect where the dissolving aluminosilicates rapidly facilitate the capture of Ca^{2+} and heavy metals into maturing

gel phases. MA presents a more complex hydraulic system, characterized by high initial contents of carbonate (15.3%), brownmillerite (9.8%), lime (6.1%), portlandite (5.2%), periclase (5.9%), and soluble alkali salts (5.3%). The leaching cycle leads to a complete dissolve of soluble salts are completely washed out, and the lime content is virtually exhausted. Concurrently, the Amorphous fraction increases from 52.6% to 59.2% in the $Ca(OH)_2$ system and as high as 67.5% in water. This increasing amorphous phase, combined with the consumption of lime, strongly implies the formation of new C-S-H hydration products. Similar to the quartz behaviour in BA, the Calcite phase in MA remains highly stable and becomes relatively enriched, rising to 22.9% of the solid residue in the CH system as more soluble components are removed. VA demonstrates the highest baseline stability, dominated by a basaltic glass phase (90.8%) with minor feldspar and olivine. After 90 days, the amorphous content remains consistently high, but a subtle transition is observed. In $Ca(OH)_2$ environments, ettringite peaks emerge, serving as characteristic crystalline indicators of the natural glass's pozzolanic transition. This proves that the volcanic glass undergoes a chemical maturation, converting from a primary vitreous state toward stable hydrated mineral form.

3.3.2 Morphological analysis

SEM coupled with EDS was used to visually confirm the microstructural evolution and the distribution of key elements (Fig. 5). Residues leached in water environment generally maintained fragmented, individual particle morphologies with clean, exposed surfaces (Fig. 5a, c, e). In contrast, particles reacted in the $Ca(OH)_2$ solution were encapsulated by a dense, pervasive layer of amorphous pozzolanic reaction products (Fig. 5b, 5d, 5f). The most compelling evidence for endogenous stabilization was found in the EDS mapping of the zinc-rich BA. As shown in Fig. 5b, the Zn signal is closely correlated with the distribution of Ca and Si within the newly formed gel layer. This proximity strongly suggests that Zn^{2+} ions are not merely trapped in a pore, but are chemically integrated into the C-A-S-H lattice or adsorbed onto its high-surface-area matrix. This reinforces our central hypothesis: the immobilization of heavy metals in these alternative SCMs is a fundamental chemical property of the pozzolanic reaction itself. By maintaining the SCM in an "unobstructed" powder state through rotation, we have proven that chemical sequestration is independent of macroscopic physical encapsulation. This distinction is vital for long-term safety assessments, as it ensures that even if the physical structure of a concrete product were to degrade, the hazardous ions remain chemically locked within the mineral phase.

3.3.3 Chemical Sequestration and Binding Orientations

Broadly, the release of heavy metals from these ashes generally aligns with the leaching behaviours of their major components [27]. A more intense dissolution reaction generally leads to a higher freedom of heavy metal ions within the system. However, over the 90-day cycle, the generation of specific mineral phases can conversely consume these ions from the solution. For instance, the pozzolanic reaction of VA in the alkaline environment results in heavy metal concentrations that are significantly lower than the pure diffusion-controlled concentrations observed in the water environment, even though early-stage dissolution was likely more vigorous. While chemisorption and physical encapsulation contribute to the immobilization of trace elements, these mechanisms are outside the scope of this study. Furthermore, while heavy metal ions may precipitate in alkaline environments due to their varying solubility products (K_{sp}), this reduction in aqueous concentration does not necessarily imply stable chemical fixation [28, 29]. Amphoteric metals like Cr are a prime example, as Cr^{6+} may exhibit higher solubility under high-pH conditions [30]. The most stable and reliable sequestration

mechanism is the direct participation of heavy metals in the hydration or pozzolanic reactions to form stable crystalline phases [31, 32]. This involves isomorphic substitution, where hazardous ions are integrated into the maturing mineral structure; for example, Cu^{2+} and Zn^{2+} can substitute for Ca^{2+}, and Cr^{3+} can replace Al^{3+}, in C-S-H gels or ettringite lattice [33–35]. The three ashes studied exhibit distinct characteristics in their endogenous binding capacity. For BA and MA, the large-scale dissolution of unstable phases combined with the release of their own alkali sources can drive an efficient ion re-capture process. However, these industrial solid wastes possess high initial heavy metal concentrations, and the reaction products (reaction sinks) they provide are apparently insufficient to fully sequester their hazardous load. In contrast, while VA in water shows a clear diffusion-controlled release of heavy metals with no plateau within 90 days, indicating a significant long-term environmental risk. It relies on stable pozzolanic reactions in alkaline environments to provide robust, long-term chemical stability.

3.4 Leaching kinetics analysis

3.4.1 Shrinking core model

The leaching kinetics of dense spherical particles in liquid can be described by the shrinking core model, which assumes that solid particles are ideal spheres [36]. The dissolution reaction rate of the solid-liquid system can be controlled by different steps and different rate equations can be derived. The rate equations of the shrinking core model are controlled by interface chemical reaction control, internal diffusion control and external diffusion control, respectively [37].

$$1-(1-\eta)^{\frac{1}{3}}=K_1 t \quad \textbf{Eq. 1}$$

$$1-\frac{2}{3}\eta-(1-\eta)^{\frac{2}{3}}=K_2 t \quad \textbf{Eq. 2}$$

$$1-(1-\eta)^{\frac{2}{3}}=K_3 t \quad \textbf{Eq. 3}$$

Where η is the leaching rate of each ions, K_1, K_2 and K_3 are the rate constant of interface chemical reaction control, internal diffusion control and external diffusion control, respectively, and t is the leaching time (min). The leaching rate η can be calculated through **Eq. 4**.

$$\eta=\frac{C_t \bullet V}{x_0 \bullet m} \quad \textbf{Eq. 4}$$

Where, C_t is the accumulative leaching concentrations, (mg/L); V is the leachate volume (L); x_0 is the metal content in raw ashes, (%); m is the mass of leaching ashes (g).

However, the elemental concentration of the solution can not be directly linked to the dissolution amount. As the dissolution going, some element would be consumed significantly if the precipitation or immobilisation reaction goes well, which lead to a decrease trend in the ICP-MS results. Among all the groups, only VA-H_2O shows a monotonic increasing trend, which can be directly explained by this SC model. As shown in Fig. 6 (a–c), all elements exhibit linear relationships in the K_2 plots, whereas the K_1 and K_3 functions show greater scatter and lower regression quality. The calculated kinetic constants and coefficients of determination (R^2) (Fig. 6d–e) consistently confirm that the internal-diffusion model (K_2) best describes the leaching behavior of all examined elements. This indicates that dissolution and element release from VA particles are primarily governed by the

diffusion of ions through an increasingly compact product layer, rather than by the surface chemical reaction at the solid–liquid interface [31]. Such a mechanism is consistent with the relatively low solubility of the volcanic glass matrix in water and the rapid formation of a silica-rich alteration film that limits further leaching. The formation of reaction products around ash grains results in diffusion as the dominant rate controlling process, especially in a later age [38]. Interestingly, the K_1 (interface-reaction) and K_3 (external-film-diffusion) fit yield almost identical slopes and R^2 values for all elements. This convergence arises because, at low leaching fraction η, the linearized K_1 and K_3 functions are mathematically parallel and nearly coincidence, as illustrated in Fig. 6 (f). Under the present rotational-batch conditions, external mass-transfer resistance is minimal; thus, the close K_1–K_3 values merely reflect this functional degeneracy near η to 0 rather than any real film-diffusion limitation.

$$\left(1-(1-\eta)^{\frac{1}{3}}\right)^2 = K_4 t \quad \textbf{Eq. 5}$$

In cementitious materials study, the models are usually expressed as Ginstling-Brounshtein equation (**Eq. 2**) and Jander equation (**Eq. 5**) [39, 40]. Ginstling-Brounshtein equation is used to characterized mass transport in the fluid layer surrounding the particles [41]. Jander equation can be used to described mass transport in the solid by-products layer. Provis also mentioned that the predictions of Ginstling-Brounshtein and Jander equation are rather similar up to a reaction extent of ~ 80%, but diverge from each other significantly after this [42]. It should also be noted that while data up to 28 days follow excellent linearity in the K_2 plots, the 90-day points deviate substantially from the trend. Therefore, the 1–28 day interval is regarded as the intrinsic diffusion-controlled window defining the baseline K_2 parameters, whereas the 28–90 day period represents a transition towards coupled diffusion–reaction behaviour. Therefore, the 1–28 day interval is considered to represent the intrinsic, diffusion-controlled regime of the VA-H_2O system, defining the baseline parameters of K2. Beyond 28 days, the observed deviations and apparent slowdown reflect a progressive coupling between diffusion and secondary reactions. These models assume a constant diffusivity and a single reaction front, which may not hold in hydrated cementitious systems where secondary precipitation and multiphase reactions occur.

3.4.2 Stage-dependent model

In order to clarify the specific leaching mechanism of each leaching stage, especially the long term stage, a stage-dependent model modified from TANK test was employed in this study [43]. The cumulative release exponent (R_c), which is the slope of log(cumulative leaching) vs. log(time), as **Eq. 8** formulated, serves as a diagnostic tool for the dominant leaching mechanism. The results are shown in **Fig. 9**.

$$\epsilon_n = \sum_{i=1}^{n} E_i (i = 1,2,3,4,5) \quad \textbf{Eq. 6}$$

$$E_i = \frac{C_i V}{A} \quad \textbf{Eq. 7}$$

$$R_c = \frac{lg\epsilon_{i+1} - lg\epsilon_i}{lgt_{i+1} - lgt_i} \quad \textbf{Eq. 8}$$

where ε_n is the cumulative leaching per unit area of the heavy metal during the leaching stages, (mg/m^2), E_i is the release amount per unit area of heavy metals in stage i, (mg/m^2). C_i is the leaching concentration tested at stage i, (mg/L). V is the volume of the leaching solution, (L). A is the surface area of the sample, (m^2). The surface area of each ash was assumed as 500 m^2/kg, which is a common value of C-class fly ash, as well as the used ashes in this study.

At the initial stage, R_c>0.65 attributed to a surface wash-off mechanism [44]. In terminal stage, when R_c>0.65, it is mainly dissolution. In any leaching period, if 0.35 < R_c<0.65, it complies with the diffusion mechanism [30, 45]. If R_c<0.35, it is conformed to depletion. In this work, as the leaching of heavy metals could decreased with the leaching time, resulted from the consuming of chemical reactions and adsorption, we took the R_c values as 0 when it less than 0, and as 1 when it higher than 1. Unlike the TANK leaching tests with periodic solution renewal, the present batch system exhibited non-monotonic concentration evolution. The negative Rc values suggest net immobilisation due to precipitation or re-adsorption (labelled as sequestration), while values exceeding 1 observed in the mid-stage indicate transient acceleration of release, likely caused by secondary dissolution of reactive phases [46]. Hence, the overall leaching behaviour is governed by chemical reaction and phase transformation rather than by pure diffusion. Accordingly, the leaching mechanism of each ash in different stages are listed in Table 2. Cu predominantly exhibits an initial depletion phase in $Ca(OH)_2$ solution, followed by diffusion or dissolution, whereas in water, it mainly follows a diffusion-dissolution pattern across different ashes. Cr leaching is primarily governed by diffusion and dissolution, with BA experiencing higher dissolution stages, indicating a more pronounced release of Cr compared to MA and VA. Mn leaching is generally controlled by depletion in the early stages, transitioning to diffusion or dissolution over time. Zn leaching demonstrates consistent diffusion-dominated mechanisms across all ashes and leachates, suggesting a more stable release pattern. Overall, the results highlight the role of ash type, metal behavior, and leachate chemistry in controlling the leaching dynamics of heavy metals. dropped significantly below 0.35, with several elements exhibiting negative R_c values (net concentration decrease) in the mid-to-late stages (28–90 d).While the standard NEN 7375 protocol interprets R_c < 0.35 as simple depletion, our "unobstructed" powder system proves it is actually driven by active chemical immobilization. In a rotation-based environment, where the ash surface area remains fully accessible, the emergence of negative R_c values is direct mathematical evidence of "reaction sinks" outcompeting the dissolution flux [47].

Table 2
Leaching mechanism of different leaching stages.

Metals	Leachate	Ashes	Stage 1	Stage 2	Stage 3	Stage 4
Cu	H_2O	BA	depletion	depletion	diffusion	depletion
		MA	sequestration	sequestration	diffusion	diffusion
		VA	depletion	diffusion	dissolution	diffusion
	$Ca(OH)_2$	BA	sequestration	sequestration	diffusion	depletion
		MA	sequestration	sequestration	diffusion	sequestration
		VA	sequestration	dissolution	dissolution	diffusion
Cr	H_2O	BA	sequestration	sequestration	diffusion	depletion
		MA	depletion	depletion	depletion	sequestration
		VA	wash-off	dissolution	dissolution	diffusion
	$Ca(OH)_2$	BA	depletion	depletion	depletion	depletion
		MA	depletion	depletion	depletion	depletion
		VA	depletion	dissolution	dissolution	diffusion
Zn	H_2O	BA	depletion	diffusion	sequestration	diffusion
		MA	sequestration	depletion	sequestration	diffusion
		VA	depletion	depletion	depletion	diffusion
	$Ca(OH)_2$	BA	diffusion	sequestration	depletion	depletion
		MA	depletion	sequestration	diffusion	sequestration
		VA	depletion	sequestration	depletion	depletion

3.4.3. Phenomenological Evidence of the "Dissolution-Sequestration" Competition

The kinetic profile of multi-source ashes in simulated cementitious pore solutions is fundamentally governed by a dynamic competition between the core's dissolution and the surface's sequestration capacity. Unlike traditional batch tests that only capture the initial "snapshot" of mobility, our long-term unobstructed test reveals a significant kinetic reversal. This behavior is consistent with the coupled dissolution–precipitation framework widely reported for cementitious systems and waste-derived materials [48, 49]. (i) In the early stages of the reaction, unstable phases within the ash undergo substantial dissolution. This vigorous initial dissolution generally leads to a higher freedom of heavy metal ions within the system, driving their early release. Such behaviour has been widely observed in alkaline leaching environments, where readily soluble or weakly bound phases dissolve rapidly [50, 51]. (ii) However, as the reaction progresses in the highly alkaline $Ca(OH)_2$ environment, the newly formed pozzolanic reaction products or hydration products act as powerful "reaction sinks". The high pH environment (≈ 12.5) not only forces the immediate precipitation of heavy metals as insoluble hydroxides, but more importantly, the maturing mineral lattice chemically integrates these hazardous

ions [52]. This occurs through isomorphic substitution, where ions like Cu^{2+} and Zn^{2+} can substitute for Ca^{2+}, and Cr^{3+} can replace Al^{3+}, in stable crystalline phases such as C-(A)-S-H gels or the ettringite lattice [53, 54].

The stage-dependent kinetic model provides direct mathematical evidence for this competition. In the mid-to-late stages (28–90 days), R_c drops significantly below 0.35, with several elements exhibiting negative R_c values, indicating a net decrease in aqueous concentration. In a rotation-based powder environment where the ash surface area remains fully accessible, the emergence of negative R_c values proves that the chemical immobilization flux of the reaction sinks outcompetes the dissolution flux. Ultimately, this transition from a dissolution-dominated regime to a sequestration-dominated one demonstrates that the pozzolanic reaction inherently possesses an endogenous capacity to chemically lock hazardous ions into its maturing mineral lattice, completely independent of the macroscopic physical encapsulation provided by a concrete monolith.

4. Conclusion

This study provides a mechanistic framework for understanding the environmental stability of multi-source ashes used as SCMs by explicitly decoupling chemical sequestration from physical encapsulation through a long-term rotation-based leaching methodology. The key conclusions are as follows:

1. In water, all ashes exhibited measurable heavy metal release, with BA showing particularly high Zn leaching (~ 10–100 mg/L). Under alkaline conditions simulating cement pore solution (pH ≈ 12.5), heavy metal concentrations decreased by 1–2 orders of magnitude, with Zn reduced to < 0.1 mg/L, demonstrating substantial intrinsic stabilization. Continuous Ca^{2+} consumption and declining conductivity confirm the formation of secondary hydrates (C-(A)-S-H, ettringite), which actively immobilize dissolved species. This establishes that ashes are not passive materials but chemically reactive systems capable of binding hazardous ions.
2. Immobilization occurs via precipitation of insoluble hydroxides and structural incorporation into hydration products through isomorphic substitution (e.g., Zn^{2+}/Cu^{2+} and Ca^{2+}, Cr^{2+} and Al^{2+}). SEM-EDS results directly confirm the integration of metals into gel phases rather than simple physical trapping. Significant dissolution of raw phases drives hydrate formation, while stable phases become relatively enriched. VA shows high intrinsic stability but relies on alkaline activation to achieve effective long-term immobilization.
3. Early-stage leaching is dominated by dissolution, while mid-to-late stages (28–90 d) show strong sequestration, evidenced by negative cumulative release exponents. This confirms that chemical immobilization can outcompete dissolution in reactive systems. In inert water systems (e.g., VA-H_2O), leaching follows diffusion-controlled behavior, whereas in reactive alkaline environments, kinetics deviate due to coupled dissolution–precipitation processes.

Overall, this work demonstrates that the long-term environmental safety of waste-derived SCMs is fundamentally controlled by their endogenous chemical reactivity rather than external physical encapsulation. The proposed methodology and mechanistic insights provide a robust scientific basis for evaluating and optimizing alternative ashes for safe, large-scale application in sustainable construction.

Declarations

Acknowledgements

This work is part of the projects: 1. Circular and climate neutral cement replacement materials industry - need for standardization, market analysis and policy making (SCM-Force), 2. Crucial transition to application of cement replacement material - A heuristic approach to identify drivers and barriers, and to propose potential solutions (SCM-Force-II).

Data availability statement

The authors declare that the data supporting the findings of this study are available within the paper and its Supplementary Information files. Should any raw data files be needed in another format they are available from the corresponding author upon reasonable request.

References

1. P.J. Monteiro, S.A. Miller, A. Horvath, Towards sustainable concrete, Nature materials, 16 (2017) 698–699.
2. B. Lothenbach, K. Scrivener, R. Hooton, Supplementary cementitious materials, Cement and concrete research, 41 (2011) 1244–1256.
3. M.C. Juenger, R. Snellings, S.A. Bernal, Supplementary cementitious materials: New sources, characterization, and performance insights, Cement and Concrete Research, 122 (2019) 257–273.
4. J. Skibsted, R. Snellings, Reactivity of supplementary cementitious materials (SCMs) in cement blends, Cement and Concrete Research, 124 (2019) 105799.
5. R. Snellings, P. Suraneni, J. Skibsted, Future and emerging supplementary cementitious materials, Cement and concrete research, 171 (2023) 107199.
6. A. Babaahmadi, G. Plusquellec, U. Mueller, Utilization of Bio Ashes in Cement-based Materials: A Case Study in Cooperation with Pulp and Paper and Energy Production Industries in Sweden, Nordic Concrete Research, 63 (2020) 63–78.
7. M.A. Munawar, A.H. Khoja, S.R. Naqvi, M.T. Mehran, M. Hassan, R. Liaquat, U.F. Dawood, Challenges and opportunities in biomass ash management and its utilization in novel applications, Renewable and Sustainable Energy Reviews, 150 (2021) 111451.
8. S.V. Vassilev, D. Baxter, L.K. Andersen, C.G. Vassileva, An overview of the composition and application of biomass ash.: Part 2. Potential utilisation, technological and ecological advantages and challenges, Fuel, 105 (2013) 19–39.
9. C. Stewart, D.E. Damby, I. Tomašek, C.J. Horwell, G.S. Plumlee, M.A. Armienta, M.G.R. Hinojosa, M. Appleby, P. Delmelle, S. Cronin, C.J. Ottley, C. Oppenheimer, S. Morman, Assessment of leachable elements in volcanic ashfall: a review and evaluation of a standardized protocol for ash hazard characterization, Journal of Volcanology and Geothermal Research, 392 (2020) 106756.
10. A. Hazarika, Characterization, Activation and Reactivity of Natural Pozzolans for Use as Supplementary Cementitious Materials, Department of Architecture and Civil Engineering, Chalmers University of …
11. A. Potysz, E.D. van Hullebusch, J. Kierczak, Perspectives regarding the use of metallurgical slags as secondary metal resources–A review of bioleaching approaches, Journal of environmental management, 219 (2018) 138–152.

12. H. Li, Z. Xu, Y. Peng, M. Xu, H. Li, Z. Han, S. Lu, J. Yan, Glycine-mediated heavy metal leaching and calcium retention from municipal solid waste incineration fly ash: A mechanistic study, Journal of Environmental Management, 387 (2025) 125928.
13. Y. Pei, M. Ike, K. Shiota, M. Takaoka, The impacts of furnace and fuel types on the hazardous heavy metal contents and leaching behavior of woody biomass fly ash, Fuel, 372 (2024) 132202.
14. T.R. Klymko, J. Dijkstra, A. Zomeren, Guidance document on hazard classification of MSWI bottom ash, ECN The Netherlands2017.
15. J. Koppejan, S. Van Loo, The handbook of biomass combustion and co-firing, Routledge2012.
16. L. Li, C. Yu, J. Bai, Q. Wang, Z. Luo, Heavy metal characterization of circulating fluidized bed derived biomass ash, Journal of Hazardous Materials, 233–234 (2012) 41–47.
17. A. Komaei, A. Moazami, H. Mirzaei, A. Soroush, Life cycle assessment of stabilization and solidification of heavy-metal contaminated sandy soil using sodium carbonate-activated volcanic ash-based geopolymer, Case Studies in Construction Materials, 22 (2025) e04776.
18. F. Faraji, A. Alizadeh, F. Rashchi, N. Mostoufi, Kinetics of leaching: a review, Reviews in Chemical Engineering, 38 (2022) 113–148.
19. S. Gao, J.-s. Li, S. Zhang, C.S. Poon, A state-of-the-art review of solid waste leaching mechanisms and evaluation methodologies, Waste Management, 204 (2025) 114941.
20. Z. Huang, K. Liu, J. Duan, Q. Wang, A review of waste-containing building materials: Characterization of the heavy metal, Construction and Building Materials, 309 (2021) 125107.
21. N. Hu, G. Chen, Y. Chen, M. Lin, P. Tang, W. Zhang, Z. Ye, Cement and zeolite stabilization/solidification of heavy metal-contaminated sediments: 841-Day leaching characteristics, mechanisms, and microstructure, Waste Management, 190 (2024) 306–317.
22. T. Zhao, H. Yang, S. Zhang, Z. Wu, The promoting effect of Fe on the immobilization of heavy metals in MSWI FA–lead–zinc tailings-based backfill materials under field application: Dynamic simulation leaching and immobilization mechanisms, Chemical Engineering Journal, 498 (2024) 155734.
23. S.J. Armistead, A. Babaahmadi, Navigating regulatory challenges, technical performance and circular economy integration of mineral-based waste materials for sustainable construction: A mini review in the European context, Waste Management & Research, (2024) 0734242X241270973.
24. M.K. Tiwari, S. Bajpai, U.K. Dewangan, R.K. Tamrakar, Suitability of leaching test methods for fly ash and slag: A review, Journal of Radiation Research and Applied Sciences, 8 (2015) 523–537.
25. V. Ettler, M. Mihaljevič, A. Culka, Contaminant release from massive copper metallurgical slags: Insights from long-term monolithic leaching tests, Chemosphere, 335 (2023) 139079.
26. E. Standrads, Methods of Testing Cement-Part 5: Pozzolanicity Test for Pozzolanic Cements, NSAI: Dublin, Ireland, (2000) 196 – 195.
27. H. Elomaa, S. Seisko, J. Lehtola, M. Lundström, A study on selective leaching of heavy metals vs. iron from fly ash, Journal of Material Cycles and Waste Management, 21 (2019) 1004–1013.
28. H. Lo, K. Lin, M. Liu, T. Pai, C. Lin, W. Liu, G. Fang, C. Lu, C. Chiang, S. Wang, Solubility of heavy metals added to MSW, Journal of Hazardous Materials, 161 (2009) 294–299.
29. W. Li, P. Ni, Y. Yi, Comparison of reactive magnesia, quick lime, and ordinary Portland cement for stabilization/solidification of heavy metal-contaminated soils, Science of the Total Environment, 671 (2019)

741–753.

30. B. Li, L. Wang, S. Jian, J. Zhang, W. Gao, J. Zhu, R. Wu, Leaching behavior of copper and chromium in the mortar containing artificial fine aggregate prepared by contaminated soil, Construction and Building Materials, 270 (2021) 121367.
31. M. Hinsenveld, P.L. Bishop, Use of the shrinking core/exposure model to describe the leachability from cement stabilized wastes, Stabilization and Solidification of Hazardous, Radioactive, and Mixed Wastes: 3rd Volume, ASTM International, 1996, pp. 528–539.
32. J. Bao, L. Wang, M. Xiao, Changes in speciation and leaching behaviors of heavy metals in dredged sediment solidified/stabilized with various materials, Environmental Science and Pollution Research, 23 (2016) 8294–8301.
33. M. Liu, Y. Zhao, Z. Yu, Z. Cao, Binding of Cu(□) and Zn(□) in Portland cement immobilization systems: Effect of C-A-S-H composition, Cement and Concrete Composites, 131 (2022) 104602.
34. S. Zhang, Y. Zhang, S. Wu, K. Yu, M. Gao, Z. Zhao, Y. Wu, Y. Zhang, Z. Zhang, Feasibility of using Cr-containing vitrification product as cement admixture: Structural evolution and chromium immobilization, Journal of Cleaner Production, 417 (2023) 138055.
35. Q. Liu, P. Feng, L. Shao, C. Chen, X. Liu, Y. Ma, L. Zhang, G. Geng, Quantifying the immobilization mechanisms of heavy metals by Calcium Silicate Hydrate (C-S-H): The case of Cu2+, Cement and Concrete Research, 186 (2024) 107695.
36. V. Safari, G. Arzpeyma, F. Rashchi, N. Mostoufi, A shrinking particle—shrinking core model for leaching of a zinc ore containing silica, International Journal of Mineral Processing, 93 (2009) 79–83.
37. Z. Quan, Z. Wang, H. Liu, Y. Ma, X. Wang, L. Zhou, C. Deng, G. Fu, Dissolution mechanism of magnesium aluminate spinel in copper smelting slag based on the shrinking core reaction models of corrosion, Materials Chemistry and Physics, 291 (2022) 126722.
38. Y. Zuo, M. Nedeljković, G. Ye, Coupled thermodynamic modelling and experimental study of sodium hydroxide activated slag, Construction and Building Materials, 188 (2018) 262–279.
39. W. Jander, W. Scheele, Reaktionen im festen Zustande bei höheren Temperaturen. X. Mitteilung. Der Reaktionsverlauf, Zeitschrift für anorganische und allgemeine Chemie, 214 (1933) 55–64.
40. A. Ginstling, The diffusion kinetics of reaction in spherical particles, J Appl Chem USSR, 23 (1950) 1327.
41. Z. Huang, Q. Wang, The effect of temperature on dissolution activity of fly ash and metakaolin in alkaline conditions, Cement and Concrete Composites, 146 (2024) 105363.
42. J.L. Provis, On the use of the Jander equation in cement hydration modelling, RILEM Technical Letters, 1 (2016) 62–66.
43. E. NEN, 7375, Leaching characteristics of moulded or monolithic building and waste materials, Determination of leaching of inorganic components with the diffusion test. The tank test, (2004).
44. H.A. van der Sloot, Leaching behaviour of waste and stabilized waste materials; characterization for environmental assessment purposes, Waste Management & Research, 8 (1990) 215–228.
45. J. Huang, D. Wang, S. Jian, B. Li, X. Gao, Pore structure characteristics and leaching mechanism of Cu and Cr in sustainable porous ceramisite produced from contaminated soil and biomass waste, Journal of Cleaner Production, 447 (2024) 141549.

46. H. Van der Sloot, J. Dijkstra, Development of horizontally standardized leaching tests for construction materials: a material based or release based approach?: Identical leaching mechanisms for different materials, ECN Petten, The Netherlands, 2004.
47. M. Chrysochoou, D. Dermatas, Evaluation of ettringite and hydrocalumite formation for heavy metal immobilization: Literature review and experimental study, Journal of hazardous materials, 136 (2006) 20–33.
48. D.S. Kosson, H.A. van der Sloot, F. Sanchez, A.C. Garrabrants, An integrated framework for evaluating leaching in waste management and utilization of secondary materials, Environmental engineering science, 19 (2002) 159–204.
49. H. Van der Sloot, Characterization of the leaching behaviour of concrete mortars and of cement–stabilized wastes with different waste loading for long term environmental assessment, Waste Management, 22 (2002) 181–186.
50. L. De Windt, R. Badreddine, Modelling of long-term dynamic leaching tests applied to solidified/stabilised waste, Waste management, 27 (2007) 1638–1647.
51. M. Dell'Orso, T. Mangialardi, A.E. Paolini, L. Piga, Evaluation of the leachability of heavy metals from cement-based materials, Journal of Hazardous Materials, 227 (2012) 1–8.
52. N. Gineys, G. Aouad, F. Sorrentino, D. Damidot, Incorporation of trace elements in Portland cement clinker: Thresholds limits for Cu, Ni, Sn or Zn, Cement and concrete research, 41 (2011) 1177–1184.
53. X. Li, C.S. Poon, H. Sun, I. Lo, D. Kirk, Heavy metal speciation and leaching behaviors in cement based solidified/stabilized waste materials, Journal of hazardous materials, 82 (2001) 215–230.
54. D. Wang, Q. Wang, Y. Cui, L. Pang, Assessing heavy-metal leaching risk in cement-industrial slag composite pastes using a mechanism-based thermodynamic approach, Cement and Concrete Composites, 140 (2023) 105074.

Figures

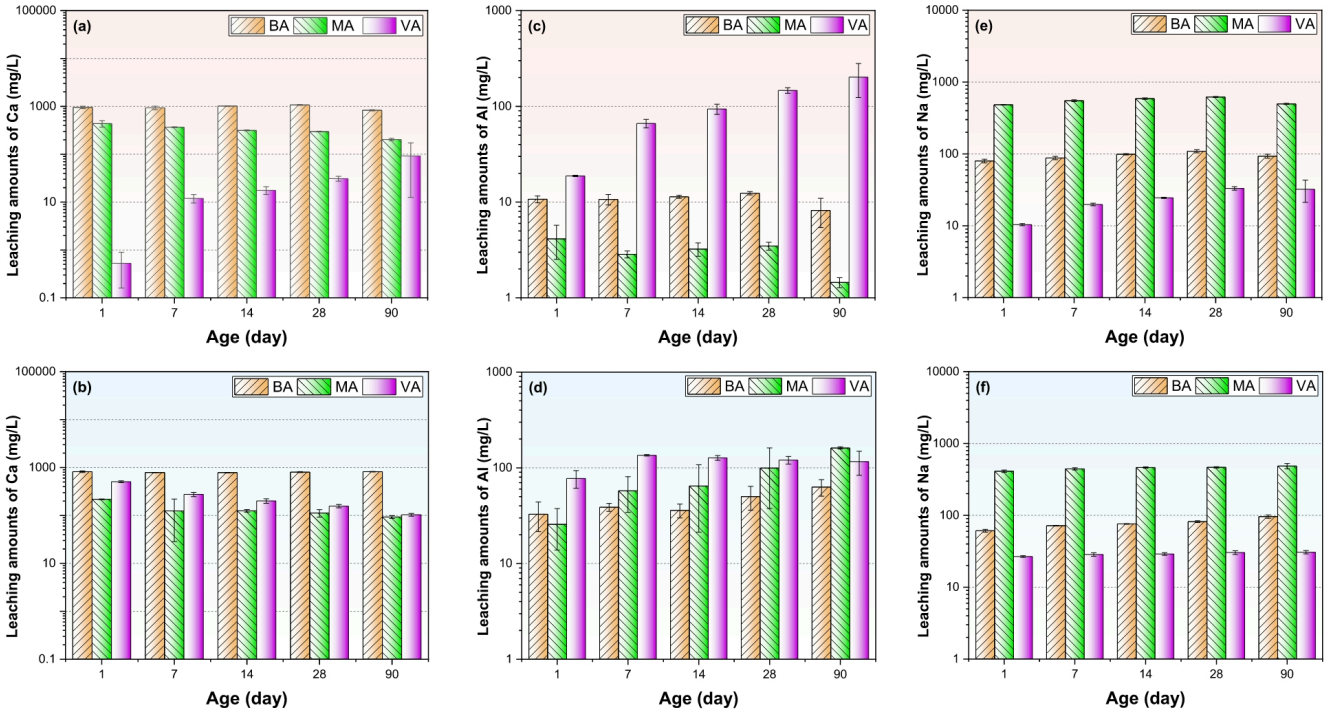


Figure 1

Leaching of major elements from different ashes, (a) Ca in water, (b) Ca in $Ca(OH)_2$ solution, (c) Al in water, (d) Al in $Ca(OH)_2$ solution, (e) Na in water, (f) Na in $Ca(OH)_2$ solution.

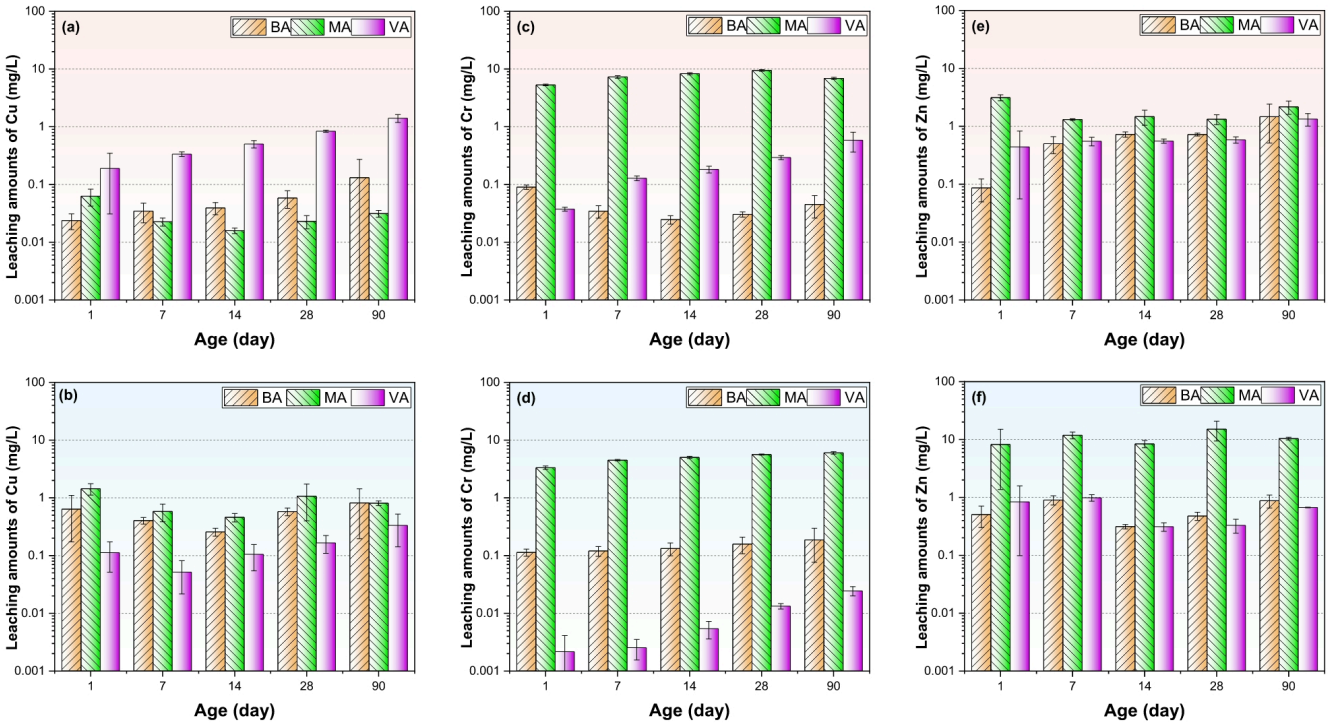


Figure 2

Leaching of trace elements from different ashes, (a) Cu in water, (b) Cu in $Ca(OH)_2$ solution, (c) Cr in water, (d) Cr in $Ca(OH)_2$ solution, (e) Zn in water, (f) Zn in $Ca(OH)_2$ solution.

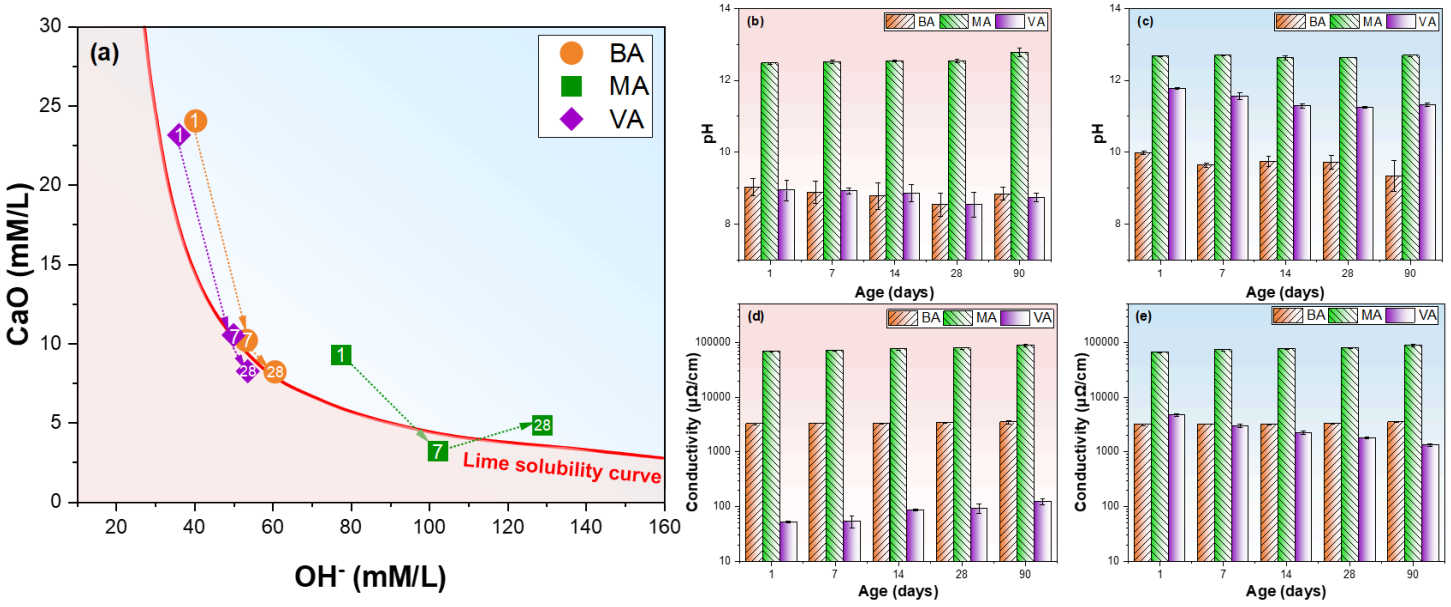


Figure 3

(a) Change in concentration of [CaO] versus $[OH]^-$ on 1, 7, and 28 days through Frattini test, (b) pH values, of leachates with different ashes in H_2O, (c) pH values, of leachates with different ashes in $Ca(OH)_2$, (d) Conductivity of leachates with different ashes in H_2O, (e) Conductivity of leachates with different ashes in $Ca(OH)_2$.

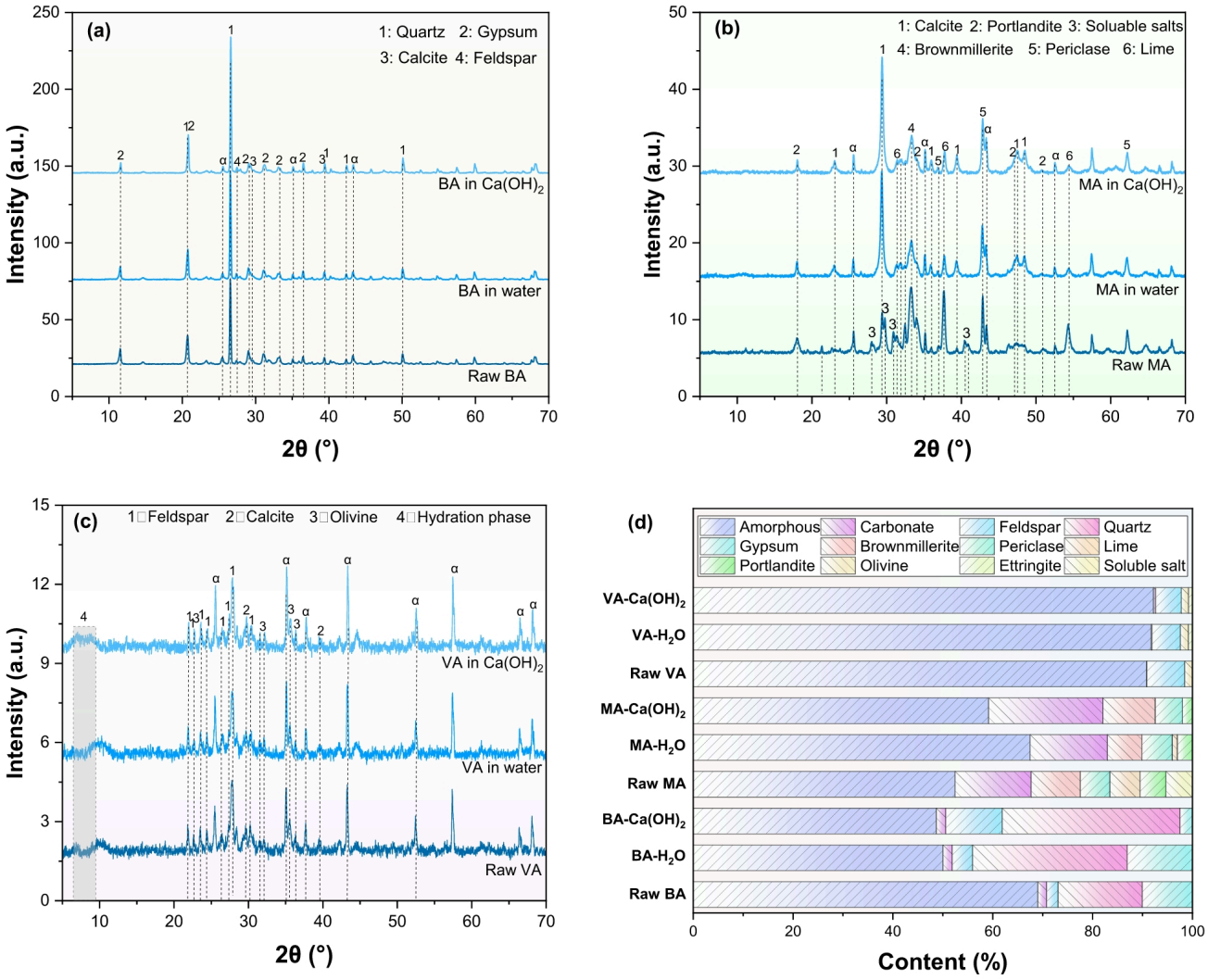


Figure 4

XRD results of each group of (a) BA, (b) MA, and (c) VA, α refers to Al_2O_3 reference peaks for quantitative comparison.

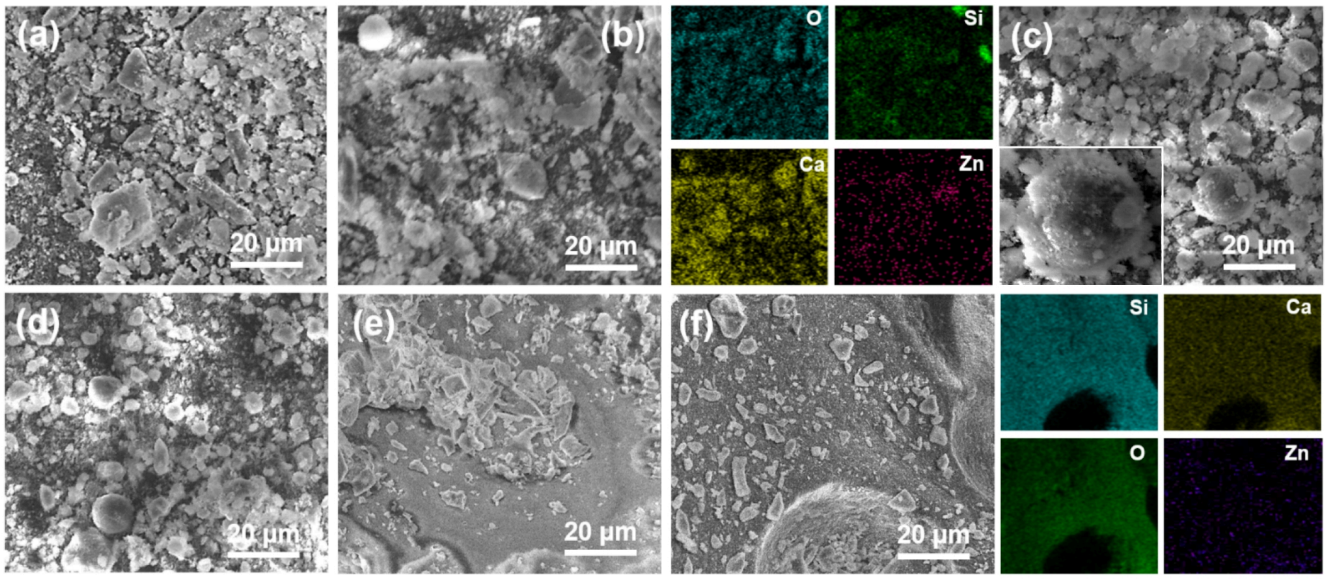


Figure 5

SEM images of (a) BA in H_2O, (b) BA in $Ca(OH)_2$, (c) MA in H_2O, (d) MA in $Ca(OH)_2$, (e) VA in H_2O, (f) VA in $Ca(OH)_2$

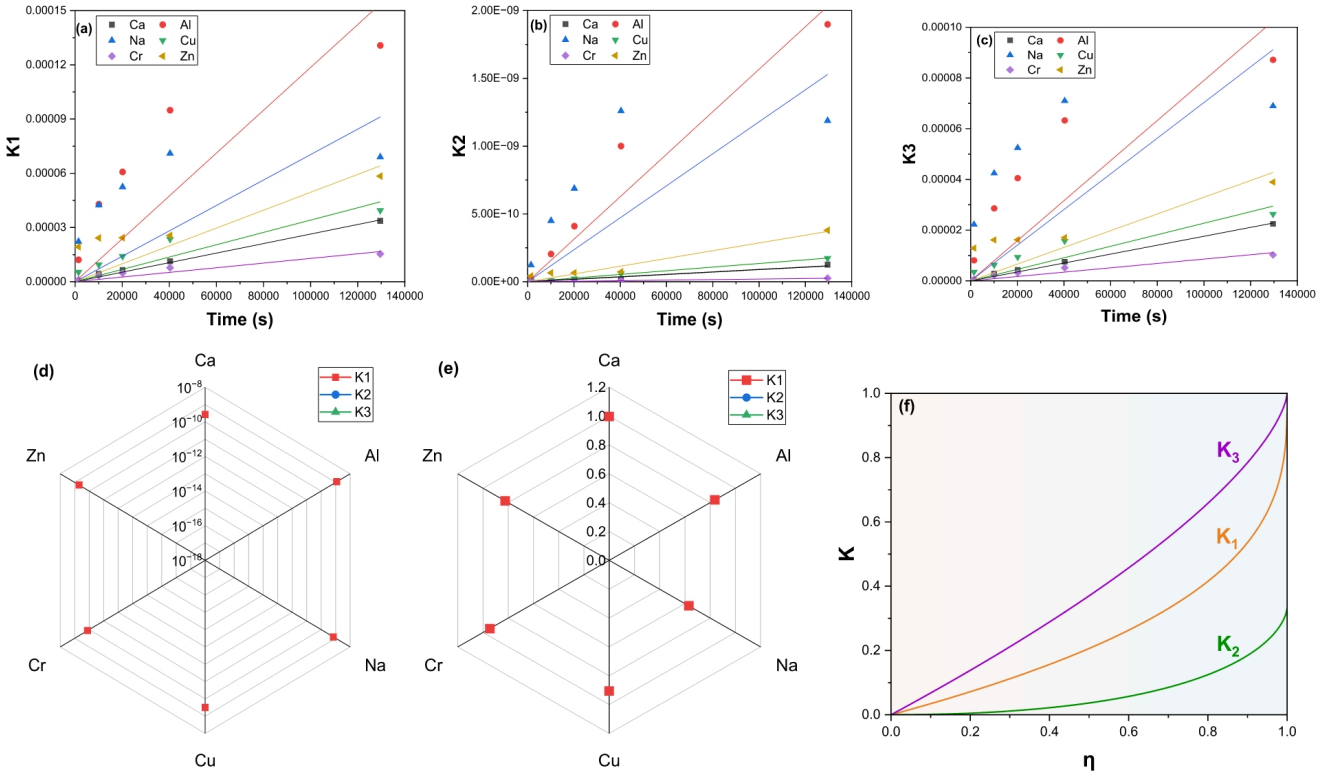


Figure 6

Fitting results (a)K1, (b) K2, (c) K3, and K values (d) and R^2 (e) obtained from fitting the leaching control mechanism.

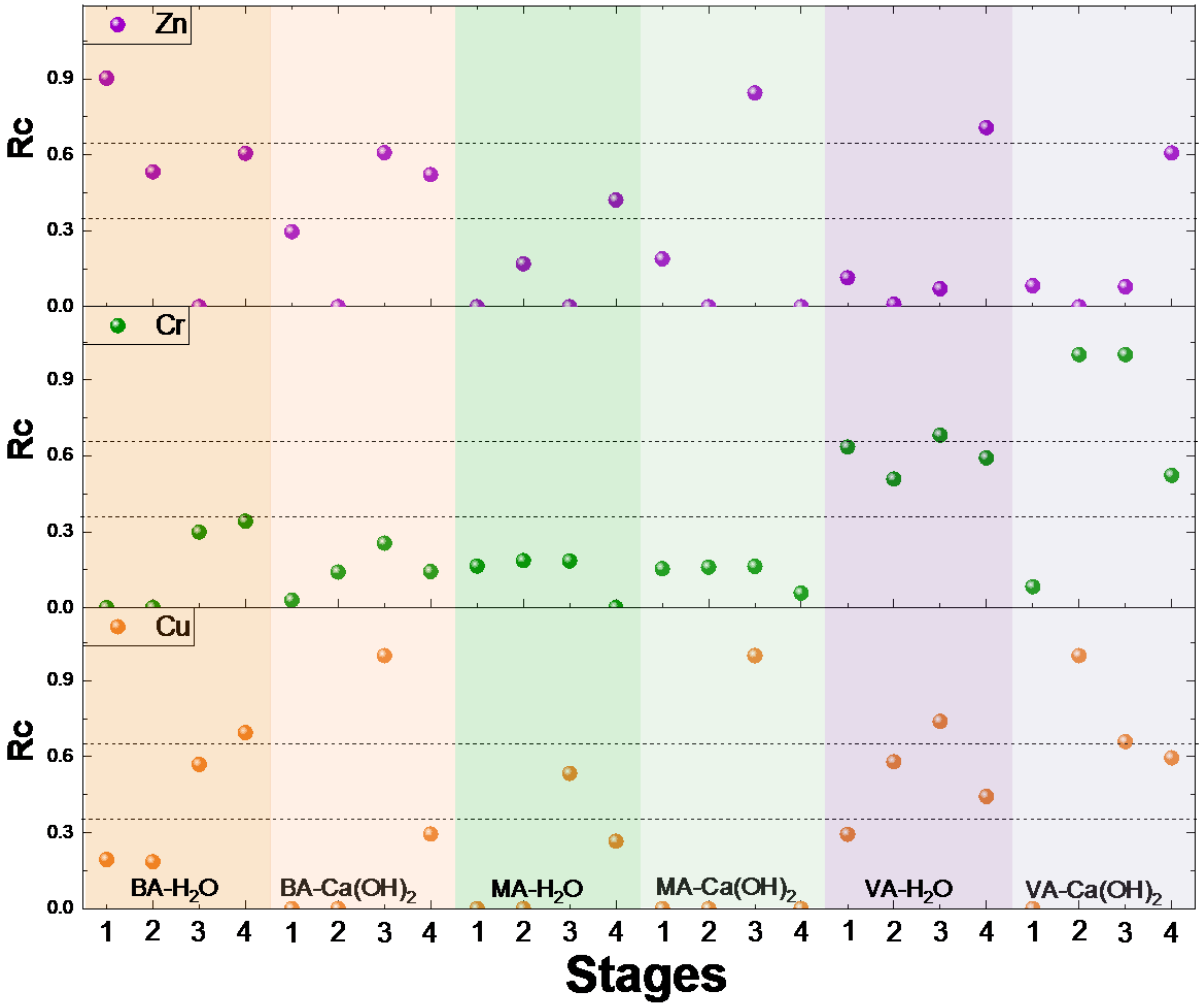


Figure 7

R_c results of different ashes.